Early Receptor Potential Evidence for the Existence of Two Thermally Stable States in the Barnacle Visual Pigment

B. MINKE, S. HOCHSTEIN, and P. HILLMAN

From The Institute of Life Sciences, The Hebrew University of Jerusalem, Jerusalem, Israel

ABSTRACT The early receptor potential (ERP) in the barnacle photoreceptor is shown by intracellular recording to exhibit a strong dependence on the color of the stimulus and of the preceding adaptation. The adaptation effects appear to be stable for at least 3 h in the dark. Most strikingly, the ERP is positive after red adaptation and mainly negative after blue adaptation. The simplest hypothesis which accounts for these observations is that two thermally stable pigment states with different absorption spectra contribute to the ERP. All ERP responses appear to be consistent with the sums of different ratios of the ERP's of the two pure states. The relative populations of the two states are shown to vary reciprocally, suggesting that the two are states of the same closed pigment cycle. Both states have approximately Dartnall nomogram-shaped absorption spectra, one peaked near 495 nm, and the other near 532 nm.

INTRODUCTION

A good deal is known (Dartnall, 1972) about the cascade of changes initiated in visual pigments by the absorption of photons. However, it has not yet been possible to isolate or even identify the stage(s) or transition(s) responsible for the membrane conductance change underlying the late receptor potential (LRP) (Arden, 1969). Many workers have attempted to correlate the LRP with the state of the pigment in various preparations. The effects of modifying this state were examined by testing cells at various times after various intensities and durations of adapting light (Dowling, 1960, 1963; Rushton, 1961, 1965; Donner and Reuter, 1967, 1968; Dowling and Ripps, 1970; Mainster and White, 1972), by testing cells after different wavelengths of adapting light (Nolte, Brown, and Smith, 1968; Hamdorf, 1970; Hamdorf, et al., 1971; Nolte and Brown, 1972), and by testing cells at various pH levels (Sillman, Owen, and Fernandez, 1972).

Nolte, et al. (1968) and Nolte and Brown (1972) suggested that an extended

dark persistent LRP observed by them derives from the presence of a metastable photoproduct. The other authors all consider that the response arises from activation of rhodopsin, with the cell sensitivity either related to the amount of unbleached rhodopsin or controlled by an additional factor, "bleached rhodopsin" or the amount or "rate of accumulation" (Sillman) of a particular photoproduct, most popularly metarhodopsin II.

Other authors who have noted the existence of long-lived metastable photoproducts, all in invertebrates, are listed in Goldsmith (1972); see also Hagins and McGaughy, 1967, Brown and White, 1972, and Tsukahara and Tasaki, 1972.

In this article we examine the early receptor potential (ERP) (Brown and Murakami, 1964) of the barnacle lateral ocellus. Although not in the causal chain to the LRP, the ERP is apparently a direct electrical manifestation of the changes in the pigment molecule which follow absorption of a photon (Cone, 1967). We have made use of the ERP to show that the barnacle pigment has a very stable photoproduct, and to establish the quantitative dependence of the pigment state populations and transitions on stimulus and adaptation wavelength, intensity, and duration. The two stable states have absorption spectra peaking at 532 and 495 nm. These wavelengths, together with the evidence given in the following article about the coupling of the activation of these states to the LRP, might suggest that the two states should be called rhodopsin and metarhodopsin, respectively. However, we shall continue to call them the 532 and 495 states since (*a*) we have no evidence as to which is more stable, (*b*) there are no biochemical data on this pigment, and (*c*) Hamdorf (1970), Schwemer et al. (1971), and other authors listed by Goldsmith (1972) and Hara and Hara (1972) refer to metastable photoproducts with absorption peaks at longer wavelength than the stable pigment.

In the following article, we examine the dependence of the LRP on the same adaptation and stimulation parameters as for the ERP. Then, by detailed comparison of the ERP and LRP dependences, we show the existence of two antagonistic contributions to the LRP arising from different portions of the pigment process and their functional dependence on pigment parameters.

A preliminary description of some of the phenomena described in these articles has been published (Hillman, Hochstein, and Minke, 1972).

METHODS

Intracellular recordings were made in excised photoreceptors of the barnacles *Balanus eburneus* and *amphitrite* as described in the preceding paper (Hillman, Dodge, Hochstein, Knight, and Minke, 1973). The color filters used here were all interference-type Balzers broad band (K-type) or narrow band (B-40-type) filters (Balzers Aktiengesellschaft, Fürstentum, Liechtenstein). The wavelength characteristics of each

filter were measured on a spectrophotometer. The total intensity emerging from the light guide at the level of the photoreceptor cell with each filter in position was measured with a radiometer. The unfiltered intensity was calculated to be about 1×10^{16} photons per cm^2 per s per nm at 550 nm at the photoreceptor, taking into account the reflectivity of the tapetum. Corneal transmittance and tapetal reflectance are high and nearly color independent (Stratten and Ogden, 1971). Table I gives, for each filter used here, the wavelength characteristics and the calculated maximum intensity at the photoreceptor. The relative accuracy of the intensity figures is about 20%, the absolute accuracy about a factor 2. Because filters are imperfect, there are components of the light intensity at all wavelengths. We have used the raw action-spectrum results (see below), and the unfiltered spectrum of light passing through the system, to calculate first-order corrections to the action spectrum points. These corrections were found to be small everywhere, reaching a maximum of 20% in the far-blue region of the spectrum.

The identification and characteristics of the ERP are discussed in detail in the preceding paper (Hillman et al., 1973). Again, most of the quantitative ERP results in this report were obtained from cells in which the LRP had disappeared spontaneously, but the qualitative ERP characteristics of the preparation were all found to be the same in the presence of the LRP, validating the application of the results to the coupling problem.

RESULTS

1. *Qualitative Observations*

The most striking observations relating to the dependence of the early receptor potential on wavelength of stimulation and of preceding adaptation are the following:

(*a*) The ERP in the barnacle photoreceptor is purely positive (intracellular recording) in a cell which has previously been adapted to red light. The ERP is purely negative at room temperature, and at least mainly negative at low temperature, in a blue-adapted cell.

(*b*) Aside from the effects of cell resistance drift, these responses are independent of the time the cell spends in the dark after the adaptation, up to at least 3 h at room temperature, after an initial short recovery period (Hillman et al., 1973).

(*c*) The sensitivity of the blue-adapted cell extends further toward the red end of the stimulus spectrum than does that of the red-adapted cell.

(*d*) No substantial differences were seen between the two species *B. amphitrite* and *eburneus*.

(*e*) We have been unable to find any substantial dependence of the ERP responses on wavelength of stimulus or adaptation in *Limulus* ventral photoreceptors (aside, of course, from the effects of the dependence of the absorption cross section on wavelength). This difference between the preparations con-

TABLE I

FILTER AND LIGHT CHARACTERISTICS

Filter	Transmission characteristics		Transmitted light
	Peak wavelength	Full width at half height	Full intensity at photoreceptor
	nm	*nm*	*photons* cm^{-2} s^{-1} × 10^{16}
Broad band			
K1	405	55	9
K2	455	65	11
K3	495	45	12
K4	555	60	46
K5	600	50	50
K6	650	55	43
Narrow band			
398	398	9	0.11
432	432	11	0.7
447	447	8	0.7
493	493	7	1.1
543	543	7	2.6
584	584	7	3.3
596	596	10	5.6
602	602	9	4.4
620	620	8	4.4
656	656	9	7

trasts with the observation that the shapes and recovery characteristics of the *Limulus* responses are very similar to those induced by white light in white-adapted barnacle photoreceptors (Hillman et al., 1973).

2. *ERP Dependence on Color Adaptation*

The adaptation dependence of the ERP is illustrated for a white-light stimulus in Fig. 1. In traces A and B the ERP is the small fast response which precedes the main positive LRP. (The LRP is somewhat reduced in this example by strong preceding light adaptation.) The ERP is isolated in C and D (in another cell) by the spontaneous disappearance of the LRP. In both cases the ERP is positive in cells previously adapted to red light (traces B and D) and is negative in blue- (or white-) adapted cells (traces A and C). (White adaptation is found to give results very similar to blue adaptation—see Discussion.)

This red-blue adaptation dichotomy persists over the entire range of temperatures tested, 0°–37°C, although the response of the blue-adapted cell becomes biphasic (positive first) at low temperatures (Fig. 1, E and see section 3). Pak and Cone (1964) and others have interpreted the disappearance of the fast positive peak with increasing temperature as arising from the speeding up of a thermal process responsible for the negative phase. Thus the fast positive

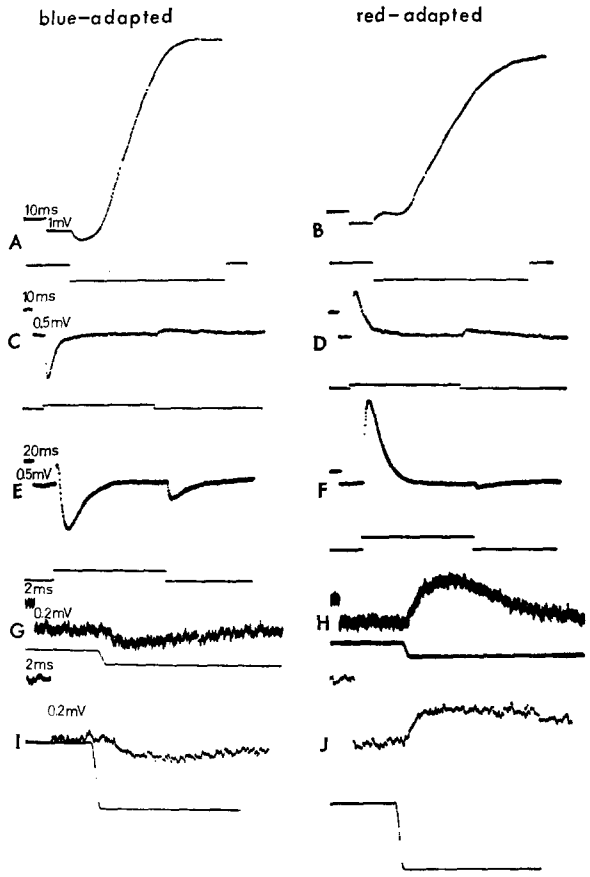

FIGURE 1. The shape dichotomy of the early receptor potential (ERP) under various conditions. All the responses are from *Balanus amphitrite*, but no qualitative differences from *B. eburneus* were found. The negative ERP elicited by white stimulation from a blue-adapted cell and the positive ERP from a red-adapted cell are shown, respectively, in the following pairs of traces: A, B, in the presence of the late receptor potential (LRP) at 24°C; C, D, after spontaneous disappearance of the LRP, 24°C; E, F, after spontaneous disappearance of the LRP, 7°C; G, H, at 24°C after suppression of the LRP by application of formaldehyde (0.6%, 10 min); I, J, at 25°C after suppression of the LRP by application of glutaraldehyde (0.6%, 10 min). The members of each pair of traces are always from the same preparation, but the pairs are all from different preparations. The calibration pulse of each trace is shown with the duration and amplitude indicated on the left traces applying as well to those on the right. The light stimulus duration is indicated in the simultaneous photocell recording below each trace. All stimuli were of full white light after 3 min in the dark after adaptation. For the left traces, the adaptation was either to blue light (15 s, 447 nm, traces C and E) or to full white light (5 s, traces A, G, and I). The effects of blue and white adaptation were almost identical. For the right traces, adaptation was to red light (620 nm, 15 s, in B, D, H, and J; K6, 15 s, in F) See Table I for filter and light characteristics. In all the figures, intensities were those given in Table I ($\log I \equiv 0$) unless otherwise indicated.

phase is canceled by the early part of the larger, but initially more slowly rising, negative phase at room temperature. The dichotomy also survives suppression of the LRP by fixation in formaldehyde (Fig. 1, G and H) or in glutaraldehyde (I and J).

The ERP shape also depends on the wavelength and intensity history of the cell adaptation. Fig. 2 shows the responses induced by fixed white stimuli after various adaptations. The center row is for saturating adaptation to the wavelengths indicated. A saturating adaptation is one for which further adaptation of the same wavelength has no further effect on the response to the

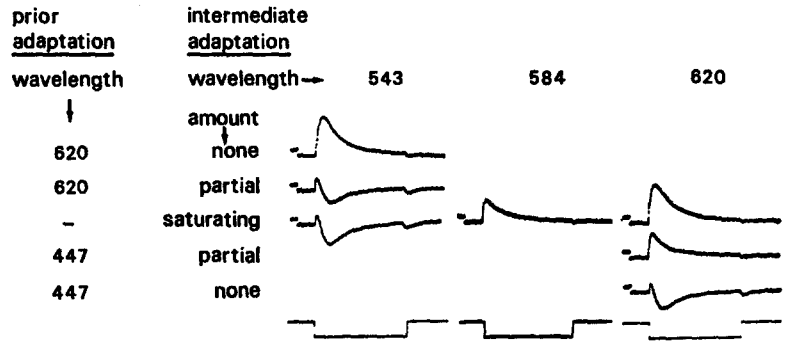

FIGURE 2. The dependence of the ERP on adaptation. *B. amphitrite*, 4°C. The responses of a single cell "prior-adapted" to saturating red (620 nm, log I = 0, 20 s) or blue (447 nm, log I = 0, 15 s) light, and readapted 30 s later to "intermediate adaptation" at 543 nm ("partial" and "saturating" are log I = −1 and 0, respectively, both 15 s), 584 nm (log I = 0, 15 s) or 620 nm ("saturating" and "partial" are log I = 0, 30 s and log I = −0.3, 15 s, respectively), as indicated. All stimuli were 250 ms of maximum white light (timing shown under each column) presented a further 30 s after the intermediate adapting light. The responses in the center row, for saturating intermediate adaptation, were independent of color of prior adaptation. The LRP had declined spontaneously in this cell. The calibration step at the beginning of each trace is 500 μV high and 20 ms long. See text.

following stimulus. The response is purely positive for any saturating adaptation above 600 nm. Below 600 nm the amplitude of the positive response begins to decrease with decreasing wavelength. A late negative peak then appears and finally all saturating adaptations below 550 nm result in predominantly negative biphasic responses (positive first) at low temperature, or purely negative responses at room temperature.

For weaker, nonsaturating, adaptations, the response shape also depends on the preceding state of adaptation ("prior" adaptation). For a given state of prior adaptation, the dependence on intensity of "intermediate" adaptation is shown in the right and left columns of Fig. 2: the top left trace shows the effect of a saturating red prior adaptation with no intermediate adaptation; the trace below it is for partial blue intermediate adaptation,

and the third trace in the column is for saturating blue intermediate adaptation. Similarly the bottom trace in the right column is for saturating blue prior adaptation, the trace above it is for partial red intermediate adaptation and the top trace in the column is for saturating red intermediate adaptation.

Fig. 3 shows that the fractional change of the response has the same dependence on adaptation amount at all times during the response. (For significance see Discussion.) The left-hand column shows responses to a fixed white test stimulus of a cell after intermediate adaptation to various amounts of blue light following prior full red adaptation. The right hand column shows the responses after the cell is intermediate adapted to various amounts of red light after prior full blue adaptation. The shape of the response is seen to change in a graded fashion with intermediate adaptation amounts. The graphs show the dependences of the logarithm of the relative change in the amplitude of the response at various times on amount of intermediate adapting light. The amplitude change at each time is plotted as a fraction of the saturated change between the responses for zero and saturating intermediate adaptation at that particular time. (To illustrate the measurement, two of the traces have copies of the traces for zero and saturating adaptations superposed on them.) Each symbol relates to a particular time after the onset of the white stimulus, and that time is indicated by the location of that symbol above the traces.

The last two traces in the left column show that intermediate adaptation of the cell with a given intensity and duration has the same effect as does adaptation with 10 times the intensity and $\frac{1}{10}$ the duration. This dependence only on the amount (intensity $\times$ duration) of intermediate adaptation was found to apply under all conditions tested.

In Figs. 2 and 3 low temperature measurements are shown since the biphasic response shapes illustrate the shape changes most dramatically. However, similar records and results were obtained at higher temperatures.

3. *ERP Shape Dependence on Wavelength of Stimulation*

The ERP depends not only on the wavelength of adaptation, but also on the wavelength of stimulation. This is illustrated in Fig. 4 at fast and slow sweep speeds in different cells in which the LRP had disappeared spontaneously.

In a red-adapted cell, all wavelengths of stimulation within the region of sensitivity elicit a purely positive response at all temperatures tested (0°–37°C) (See for instance fast and slow traces of third row of Fig. 4 and traces D and F of Fig. 1 at 3°, 5°, 24°, and 7°C, respectively). At any temperature, the shape of the response to *weak* stimuli, or of the early part of the response to stronger stimuli, is the same for all stimulus wavelengths. (Two responses are said to have the same shape if they differ only by an amplitude scale factor. The reason the stimulus must be weak, or only the early part of the response

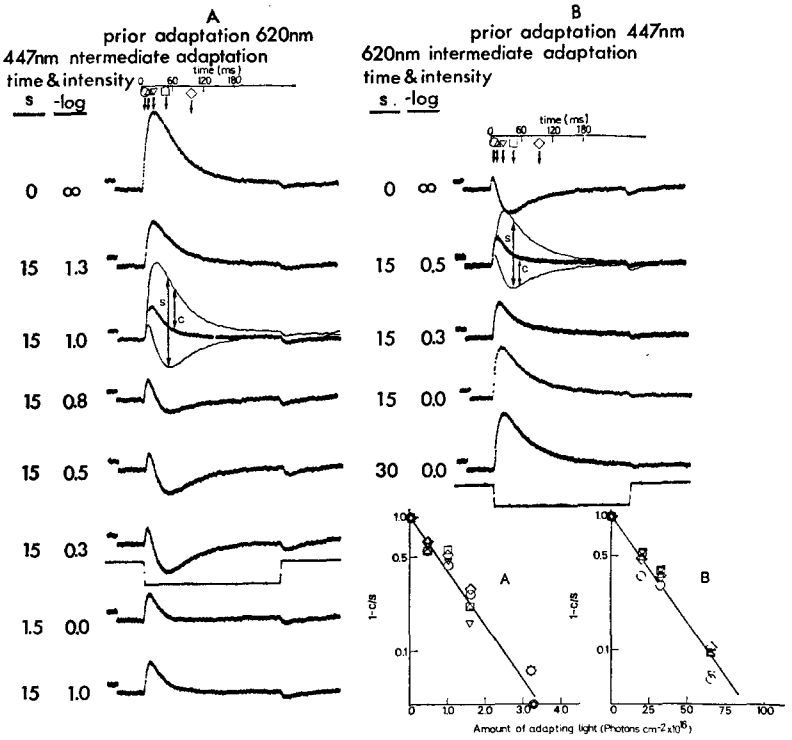

FIGURE 3. The dependence of the ERP on amount of intermediate adapting light. *B. amphitrite*, 4°C. For columns A and B, respectively, a cell received strong red (620 nm, 20 s) or blue (447 nm, 15 s) prior adaptation. After 30 s in the dark, the cell was given partial intermediate adaptation to blue (447 nm) or red (620 nm) light of various intensities and durations as indicated. Finally, after a further 30 s dark period, the cell was tested with a full intensity white stimulus (duration indicated by photocell recording shown below each series). The traces show the ERP responses to this stimulus. The last two traces in column A show that the effects of intermediate adaptation of the cell for 15 s at intensity log $I = -1.0$ are the same as the effects of intermediate adaptation of $\frac{1}{10}$ the duration and 10 times the intensity. The conditions for the last trace of column B are effectively the same as those for the first trace of column A, but the measurement was carried out 2 h later. The relative decrease in amplitude of the former reflects the decline of the cell resistance during this time. The calibration step at the beginning of each trace is 500 μV high and 20 ms long. The dependence of cell adaptation state on amount of intermediate adapting light is tested by the relative heights of the responses, after different amounts of intermediate adaptation. The response height is measured at selected times after the start of the stimuli as indicated by the positions of the symbols above the series of responses. The graphs plot the logarithms of 1 minus the changes in the response height at each time (as fractions of the saturated change at that time) against amount of intermediate adapting light for the two columns, respectively. For example, copies of the top and sixth (fifth) intermediate adaptation responses of the left (right) series are superimposed on the third (second) response in that series. The arrows indicate the response height change, c, and the saturated change, s, at one chosen time.

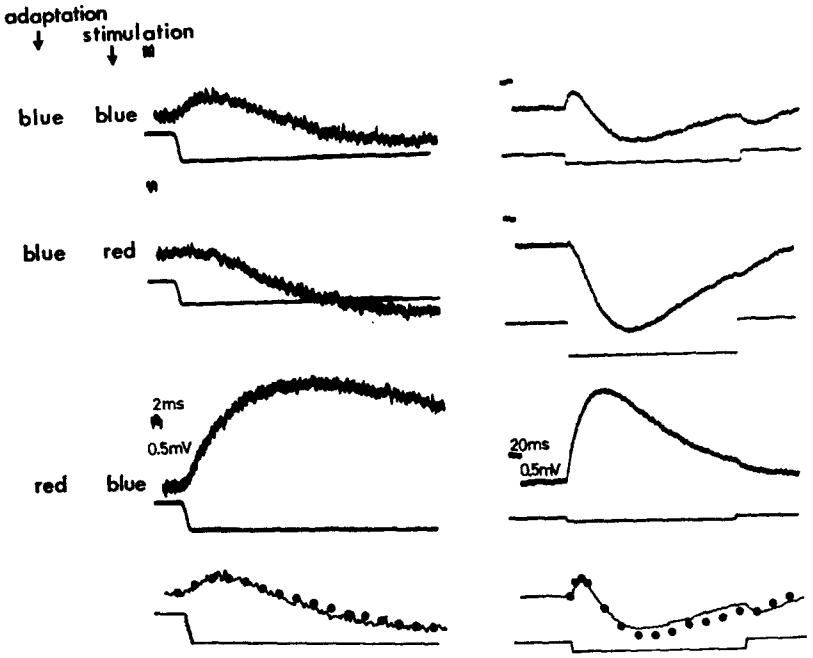

FIGURE 4. Fast and slow recordings of biphasic and monophasic negative and positive ERP shapes. (First column, 3°C, *B. amphitrite*; second column, 5°C, *B. eburneus*). The top row shows the biphasic response to blue stimulation (K3) after 1 min in the dark after strong adaptation to blue light (K3, 5 s). The second row shows the monophasic negative response to red stimulation (K5) after 1 min in the dark after strong adaptation to blue light (K3, 5 s). The third row shows the monophasic positive response after red adaptation (620 nm, 20 s) in this case to blue stimulation (K3), though the shape is maintained for any wavelength of not too strong stimulation (see text). Initial calibration steps for each column are all of the duration and amplitude indicated in the third row. The stimulus durations, simultaneously recorded by a photocell, are shown below each trace (the gain was varied, however, during the experiments). The bottom row is a copy of the biphasic response of the top row, and on it are superimposed points which are the weighted sums of the monophasic negative responses (weighting for both traces 0.9) and the monophasic positive responses (weighting 0.3 and 0.5 for the fast and slow traces, respectively). These weightings were chosen to give a best fit of the points to the curves. See text.

examined, is to ensure that the state of the cell not change appreciably during the stimulus. This is necessary since stimuli of different wavelengths will in general affect the cell in different ways. We showed that this requirement was fulfilled by checking that if the same stimulus was applied twice in succession, with an interval short compared with the ERP recovery time [preceding article], the response to the second stimulus was nearly the same as to the first).

The shape of the response of the blue-adapted cell is *not* independent of

stimulus wavelength. At low temperatures, in particular, the ratio of the peak amplitudes of the positive and negative components of the biphasic responses (Fig. 4, top row) decreases for stimuli above 550 nm and approaches zero (pure negative response) for stimuli above 600 nm (Fig. 4, second row). The initial rise of this pure negative response is slow at low temperatures and becomes faster with increasing temperature. This explains the disappearance of the fast positive peak in the response to stimuli below 600 nm at room temperature. However, the canceled positive contribution continues to influence the response shape, causing a stimulus-wavelength-dependent variation in the shape of the purely negative response at room temperature. The shape of the response to all weak stimuli is the same for all wavelengths above 600 nm.

4. *Relationship among ERP Shapes*

We have found that it is possible to reproduce the shapes and amplitudes of the ERP responses of a cell in any state of adaptation and to any wavelength and *low* intensity of stimulation (or to reproduce the early parts of responses to stronger stimuli) with the weighted sums of only two basic shapes: (*a*) that of the pure positive responses to weak stimulation of the same cell (at the same temperature) when red-adapted (these shapes are the same for all wavelengths of stimulation, as noted above); and (*b*) that of the pure negative response of the blue-adapted cell to weak stimulation above 600 nm.

The bottom row of Fig. 4 shows two typical calculations. The points represent the weighted sum of the "pure" negative and positive responses of the second and third rows, respectively (for the two columns separately), with the weighting parameters chosen for best fit to the responses of the top row (traced). The example chosen is for low temperature where the shape depends most strongly on wavelength of stimulation.

5. *The Criterion Action Spectra*

One of the most useful ways of establishing the origin of various responses of a system to light, or at least of determining if they have a common origin, is the examination of their action spectra (Brown, Murray, and Smith, 1967; Carr and Siegel, 1970; Cone, 1964; Gedney et al., 1971; Goldstein, 1967; Pak and Cone, 1964; Pak and Ebrey, 1966). The classical "criterion action spectrum" is the wavelength dependence of the reciprocal of the stimulus intensity needed at each wavelength to produce a criterion response shape and size. The stimulus must be weak, as defined and for reasons given above.

In the red-adapted barnacle photoreceptor, it was (as noted above) possible to match the shape and size of a criterion purely positive ERP response (or, for stronger stimuli, of the early part of this response) at all stimulus wavelengths within the range of sensitivity. Test stimuli of the given wavelength and with various intensities were presented to the cell until the response (or its

early part) matched the chosen criterion. The cell was readapted to red light between each test. The reciprocal of the intensity required for that match is the sensitivity at that wavelength. The action spectrum is the wavelength dependence of that sensitivity. Measurements at 8° and 22°C showed no systematic temperature dependence. Determinations from three cells, separately normalized to 1 at their peaks, were averaged and the results are the open circles in Fig. 5. The normalization is necessary since the arbitrary choice of criterion amplitude makes the intensity scale arbitrary for each cell. A Dartnall nomogram (Dartnall, 1953) peaked at 495 nm and also normalized to 1 at its peak is shown for comparison. Selected measurements indicate that the results are independent of the chosen criterion amplitude, within the region explored, a range of about a factor 10.

Because of the linearity of the ERP (Fig. 2 of preceding article), one should get the same shape of action spectrum by plotting, instead, amplitudes elicited by a constant quantum flux. Sample measurements indicated this to be correct.

For the blue-adapted cell it was, also as noted above, *not* possible to match the same criterion response shape and size at different stimulus wavelengths, except within the region above 600 nm. Since the response at room temperature remained purely negative, and at low temperature mainly negative, at all stimulus wavelengths, the intensity needed to produce a criterion peak negative *amplitude* was nevertheless determined at each wavelength, even if the *shape* varied. The results, also the averages of three separately normalized experiments, are plotted as the crosses in Fig. 5. A Dartnall nomogram peaked at 532 nm is shown for comparison.

However, we showed in the preceding section that the shape change in the blue-adapted cell probably arises from different relative contributions, at different wavelengths, of the "pure" positive and negative responses. It is possible to extract the "pure" negative ERP action spectrum from the responses of the blue-adapted cell. One method of doing so is the extraction of the pure negative component of the biphasic ERP by superposition as in the bottom of Fig. 4. The fraction of the full negative response needed at each wavelength reflects the action spectrum of this component. The triangles plotted in Fig. 5 are derived in this way, as detailed in the Appendix.

DISCUSSION

If the ERP is a direct manifestation of a pigment process, it is clear from the ERP shape dependence upon wavelength of adaptation and stimulation that barnacle photoreceptor pigment has at least two stable states. The stability of those states is shown by the independence of the ERP on time in the dark, after the initial rapid recovery discussed in the preceding article. All responses to weak stimulation may be reproduced by the weighted sums of two basic

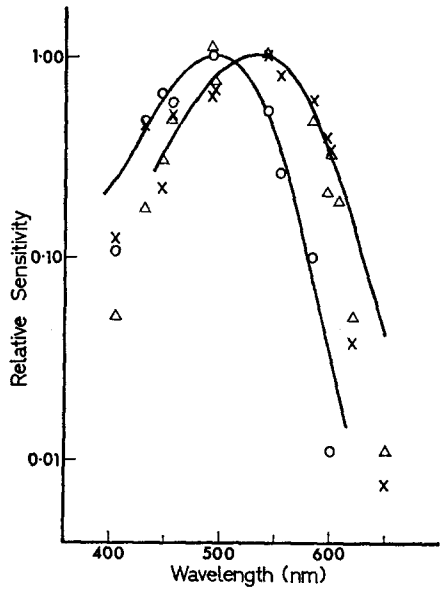

FIGURE 5. ERP criterion action spectra. *B. amphitrite*. Each circle is the reciprocal of the relative number of photons required at the corresponding wavelength on the abscissa to elicit a criterion shape and size of (positive) ERP from a cell which had been adapted 2 min earlier to strong red light (K6, 10 s). Each cross is the reciprocal of the relative number of photons required at that wavelength to elicit a criterion *negative amplitude* of ERP from a cell which had been adapted 2 min earlier to strong blue light (447 nm, 10 s) (see text). All points are averages of two determinations at 8°C and one at 22°C; no systematic dependence on temperature was found. Both narrow and broad band filters were used. Each triangle is the fraction of the pure negative response which when summed to the correct fraction of the pure positive response gave the mixed state response at the corresponding wavelength, corrected for light intensity, as calculated in the Appendix. Four independent measurements in two different cells were normalized to one another at 600 nm and then averaged. Dartnall nomograms with peaks at 495 and 532 nm are given for comparison. All sets of points and both nomograms are normalized to 1 at their peaks, or in the case of the triangles, at the 543 nm point.

response shapes (Fig. 4 and Appendix) indicating that there are not more than two stable states. Variable weighting is necessary for both basic responses suggesting that the populations of both states vary with adaptation. The fractional change of the response has the same dependence on adaptation amount at all times during the response (Fig. 3). Since the ERP's due to the activation of the two states have different time-courses (especially at low temperature—Fig. 4) this indicates that the two states approach their new populations at the same rate—that is vary reciprocally—and hence are most probably two states of the same pigment which are photochemically interconverted.

The observation that stimulation of a red-adapted cell with light of any

wavelength, in the sensitive region of the spectrum, gives the identically shaped (purely positive ERP) response indicates that the pigment in a red-adapted cell is overwhelmingly in one state. The criterion action spectrum for this state is thus the action spectrum of the red-adapted cell, peaking at 495 nm. We call this state of the pigment the 495 state.

The variation of the ERP shape in a blue-adapted cell with stimulus wavelength indicates that both states are populated. By subtraction of the 495 state (positive ERP) component from this mixed response, we are able to compute the action spectrum of the remaining (negative) component (Appendix). This peaks near 532 nm and hence we call this state the 532 state. This spectrum is similar to that directly measured in the blue-adapted cell, as would be expected since the 532 population fraction in such cells is generally fairly high. This fraction, as derived from the decomposition calculation, was mostly in the range 0.7–0.9; in one case only, down to 0.5. Because of the shapes of the spectra, the 532 to 495 cross-section ratio above 600 nm is very large, while the 495 to 532 cross-section ratio in the region below 550 nm is smaller. This is the reason that nearly all the pigment in a red-adapted cell is in the 495 state while in the blue-adapted cell only 70–90% is in the 532 state. (The fact that the 532 cross section is both dominant and appreciable only in a very narrow wavelength region explains why the results of white adaptation are very similar to those of blue adaptation.) The determination of the population ratio quantitatively involves factors other than the cross-section ratios, however, since the pigment system involves multiple unstable states in addition to the two stable states, as will be shown elsewhere.

CONCLUSION

We thus conclude that the barnacle photoreceptor contains a single ERP-active visual pigment with two thermally stable states; that activation of one peak a purely positive ERP; that this state has an absorption spectrum with a gives near 495 nm and a shape approximating a Dartnall nomogram; that activation of the second state gives a purely negative ERP; and that this state has an absorption spectrum with a peak near 532 nm and which is also approximately Dartnall nomogram-shaped. The initial rate of rise of the negative ERP depends on temperature and at low temperatures it is slower than that of the positive ERP. Simultaneous activation of both states therefore yields a biphasic ERP at low temperatures.

The difference between the absorption spectra of the two stable states makes it possible to manipulate their relative populations by appropriate adaptation. The stable state population divisions resulting from particular adaptations can be calculated from decomposition of the response to a following test flash as detailed in the Appendix. The net amount of pigment transferred from one state to the other by a particular stimulation after a particular

adaptation can thus be quantitatively determined. It is convenient for purposes of comparison with the LRP in the following article, to call the degree of population shift resulting from a particular adaptation-stimulation combination the degree of "reddening" of the cell, if the population shift is from the 532 to the 495 state, and "blueing" if the reverse. A stimulus is "neutral" if it leaves the final populations unchanged.

A stimulus is thus "neutral" if it is of the same color as the preceding saturating adaptation or nearly neutral if both are below 550 nm or above 600 nm. A stimulus is "reddening" if it is of longer wavelength than the preceding saturating adaptation; the degree of reddening depends on the extent to which this shift spans the range 550–600 nm. A stimulus is "blueing" if it is of shorter wavelength than the preceding saturating adaptation; the degree of blueing again depends on the extent to which this shift spans the range 550–600 nm.

In the following article, we show that antagonistic LRP phenomena are induced by reddening and blueing stimuli, respectively, and that the strengths of these effects are directly proportional to the degrees of reddening and blueing of the pigment. We shall therefore conclude that antagonistic LRP processes arise from different specific stages of the pigment process responsible for the ERP in this preparation.

APPENDIX

Derivation of 532 State Action Spectrum

We derive the action spectrum of the 532 state of the barnacle pigment using the action spectrum of the 495 state and the responses of a blue-adapted cell. As noted in the text, blue adaptation puts most but not all of the pigment into the 532 state, while red adaptation puts almost all the pigment into the 495 state. The shape of the 495 state response and its dependence on stimulus wavelength (the 495 action spectrum, Fig. 5) are thus easily obtained as described in the text. The shape of the 532 state response is that of the response of the blue-adapted cell to red light (see text). Using this information, the mixed responses of the blue-adapted cell to other wavelengths can be resolved into the contributions of the 495 and 532 states as shown in Fig. 4. Here, however, we use a computer to calculate a simultaneous least-squares best-fit for the mixed responses at low temperature to a complete set of stimuli in the entire effective range of visible wavelengths. The low temperature responses were chosen because the difference between the time scales of the two contributions is amplified at low temperature, increasing the accuracy of the decomposition.

We attempt to match the amplitude of the mixed response at each time during its course, to the weighted sum of the amplitudes of the contributions of the 495 and 532 states at the same times after the start of the respective stimuli. The weightings reflect the different activations of both states resulting from different populations (different adaptation states) and different stimulus wavelengths (different absorption cross sections) and intensities. We factor the weightings into their dependences on

these three factors: state of adaptation, absorption cross section, and intensity. Thus we set

$$M(w, a, t) = P(w, a, t) + N(w, a, t)$$

$$= \frac{f_P(a)}{f_P(a')} \frac{I(w)}{I(w')} \frac{S_P(w)}{S_P(w')} P(w', a', t) + \frac{f_N(a)}{f_N(a'')} \frac{I(w)}{I(w'')} \frac{S_N(w)}{S_N(w'')} N(w'', a'', t),$$

where $M(w, a, t)$, $P(w, a, t)$, and $N(w, a, t)$ are the amplitudes of the mixed responses and those of the pure 495 and 532 states, respectively, all at the same chosen time t after the start of the respective stimuli, of intensity I, at wavelength w, of the cell in state a. (This state is directly modulated by light history, but may also be influenced by temperature, metabolic state, etc.) P can be directly measured only for a' corresponding to red-adaptation; and N can be directly measured only for a'' and w'' corresponding to blue adaptation and red stimulation. $S_P(w)$ and $S_N(w)$ are the cross sections of the 495 and 532 states, respectively, at the wavelength w.

We may simplify our calculation by measuring the 495 response for the same stimulation wavelength as the mixed response ($w' = w$) and by measuring the 532 response for the same state of *adaptation* as the mixed response ($a'' = a$) so that

$$M(w, a, t) = \frac{f_P(a)}{f_P(a')} P(w, a', t) + \frac{I(w)}{I(w'')} \frac{S_N(w)}{S_N(w'')} N(w'', a, t).$$

Alternatively, we may use the time-course of one typical, or some average, $P(w', a', t)$ and the previously determined action spectrum for the 495 state, to obtain

$$P(w, a', t) = \frac{I(w)}{I(w')} \frac{S_P(w)}{S_P(w')} P(w', a', t).$$

Both methods were in fact used, with similar results.

Furthermore, in any one set of experiments, measurements were made over the full range of wavelengths but the states of adaptation a and a' were kept constant, so that $f_P(a)/f_P(a')$ was constrained in the computer calculation to maintain a constant value.

This calculation assumes that the pigment state populations remain approximately constant during the stimulus. Using the testing technique described in the Methods section of the preceding article, we determined that stimuli of duration longer than about 30 ms began appreciably to affect the populations in the case of the stronger stimuli. The stimuli used for the calculations were of longer duration, but only the first 24 ms of every response were used for the computer fit. The calculated and experimental curves in fact diverge strongly, in the worst case, after 30 ms.

Fig. 6 shows one set of computer best-fits. Here the value of $f_P(a)/f_P(a')$ was found to be 0.2. [This value is actually a close approximation to $f_P(a)$, since $f_P(a')$ is always near 1.] The values of $S_N(w)/S_N(w'')$ matched, within an experimental error of 0.1 log unit, those of other sets of measurements where $f_P(a)/f_P(a')$ was found to be different (the range was 0.1–0.3 and in one case 0.5). The sensitivity measure-

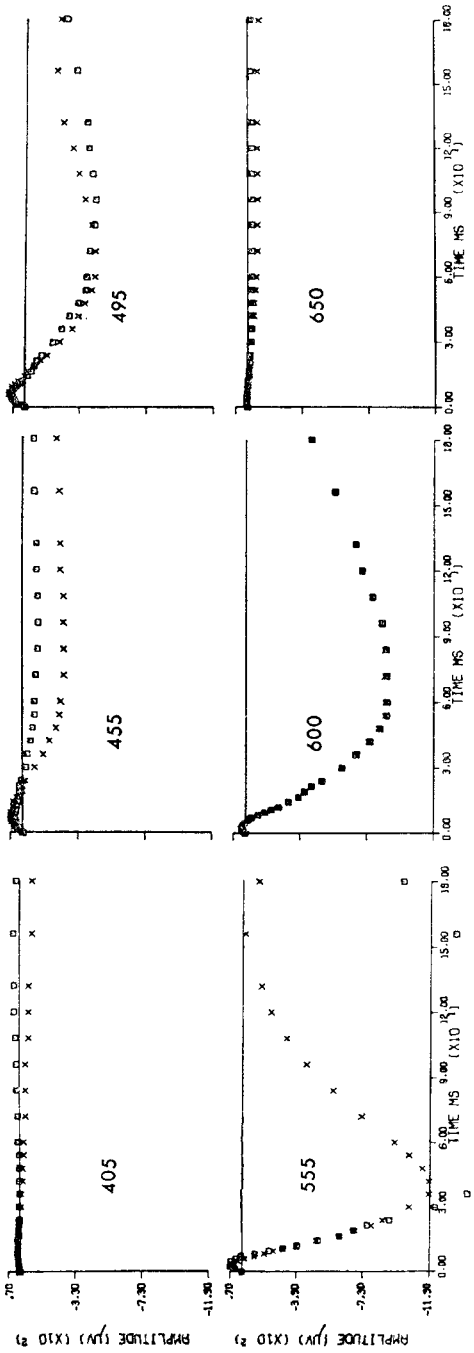

FIGURE 6. Computer fits of sums of the "pure" responses to the mixed responses. The crosses represent the observed responses of a blue-adapted cell (447 nm, 10 s) to stimuli of various wavelengths. (Peak transmission wavelength indicated: the filters were respectively K1, 2, 3, 4, 5, and 6; see Table I.) The squares are sums of fractions of the responses, to the same stimuli, of the same cell when red-adapted, with fractions of the responses of the blue-adapted cell to K5 stimulation as shown. See Appendix.

ments (four determinations in two cells) were averaged and the averages are plotted as triangles in Fig. 5. In one set of measurements the narrow-band filters gave rather weak responses, and $f_P(a)/f_P(a')$ for this set was pre-fixed at the value derived from the fit to the broad-band measurements on the same cell. A Dartnall nomogram peaking at 532 nm is shown for comparison (a good fit was obtained in the range 527–537 nm). The nomogram at its peak and the results at the 543 nm point, are normalized to 1.

This means of determining the negative ERP action spectrum clearly does not involve matching a criterion response. However, the linearity of the ERP validates the method.

We warmly thank Professors H. Mendlowitz, I. Parnas, and especially R. Werman for discussions and for critical readings of the manuscript. Miss H. Simhai's technical assistance was most useful. This research was supported in part by a grant from the Central Research Fund of the Hebrew University.

Received for publication 17 April 1972.

REFERENCES

ARDEN, G. B. 1969. The excitation of photoreceptors. *Prog. Biophys. Mol. Biol.* **19**:373.

BROWN, J. E., J. R. MURRAY, and T. G. SMITH. 1967. Photoelectric potential from photoreceptor cells in ventral eye of *Limulus*. *Science* (*Wash. D. C.*). **158**:665.

BROWN, K. T., and M. MURAKAMI. 1964. A new receptor potential of the monkey retina with no detectable latency. *Nature* (*Lond.*). **201**:626.

BROWN, P. K., and R. H. WHITE. 1972. Rhodopsin of the larval mosquito. *J. Gen. Physiol.* **59**:401.

CARR, R. E., and I. M. SIEGEL. 1970. Action spectrum of the human early receptor potential. *Nature* (*Lond.*). **225**:88.

CONE, R. A. 1964. Early receptor potential of the vertebrate retina. *Nature* (*Lond.*). **204**:736.

CONE, R. A. 1967. Early receptor potential: photoreversible charge displacement in rhodopsin. *Science* (*Wash. D.C.*). **155**:1128.

DARTNALL, H. J. A. 1953. The interpretation of spectral sensitivity curves. *Br. Med. Bull.* **9**:24.

DARTNALL, H. J. A., editor. 1972. Handbook of Sensory Physiology. Vol. VII/1, Photochemistry of vision. Springer-Verlag, Berlin.

DONNER, K. O., and T. REUTER. 1967. Dark-adaptation processes in the rhodopsin rods of the frog's retina. *Vision Res.* **7**:17.

DONNER, K. O., and T. REUTER. 1968. Visual adaptation of the rhodopsin rods in frog's retina. *J. Physiol.* (*Lond.*). **199**:59.

DOWLING, J. E. 1960. The chemistry of visual adaptation in the rat. *Nature* (Lond.). **188**:114.

DOWLING, J. E. 1963. Neural and photochemical mechanisms of visual adaptation in the rat. *J. Gen. Physiol.* **46**:1287.

DOWLING, J. E., and H. RIPPS. 1970. Visual adaptation in the retina of the skate. *J. Gen. Physiol.* **56**:491.

GEDNEY, C., J. WARD, and S. E. OSTROY. 1971. Isolation and study of rhodopsin and cone responses in frog retina. *Am. J. Physiol.* **221**:1754.

GOLDSMITH, T. H. 1972. The natural history of invertebrate visual pigments. *In* Handbook of Sensory Physiology. Vol. VII/1, Photochemistry of Vision. H. J. A. Dartnall, editor. Springer-Verlag, Berlin.

GOLDSTEIN, E. B. 1967. Early receptor potential of the isolated frog (*Rana pipiens*) retina. *Vision Res.* **7**:837.

HAGINS, W. A., and R. E. MCGAUGHY. 1967. Molecular and thermal origins of fast photoelectric effects in the squid retina. *Science* (*Wash. D. C.*). **157**:813.

HAMDORF, K. 1970. Correlation between the concentration of visual pigment and sensitivity in photoreceptors. *Verh. Dtsch. Zool. Ges.* **64**:148.

HAMDORF, K., M. GOGALA, and J. SCHWEMER. 1971. Accelerations of dark-adaptation by visual light in UV-receptors. *Z. Vgl. Physiol.* **75**:189.

HARA, T., and R. HARA. 1972. Cephalopod retinochrome. *In* Handbook of Sensory Physiology. Vol. VII/1, Photochemistry of Vision. H. J. A. Dartnall, editor. Springer-Verlag, Berlin.

HILLMAN, P., F. A. DODGE, S. HOCHSTEIN, B. W. KNIGHT, and B. MINKE. 1973. Rapid recovery of invertebrate early receptor potential. *J. Gen. Physiol.* **62**:77.

HILLMAN, P., S. HOCHSTEIN, and B. MINKE. 1972. A visual pigment with two physiologically active stable states. *Science* (*Wash. D.C.*). **175**:1486.

HOCHSTEIN, S., B. MINKE, and P. HILLMAN. 1973. Antagonistic components of the late receptor potential in the barnacle photoreceptor arising from different stages of the pigment process. *J. Gen. Physiol.* **62**:105.

MAINSTER, M. A., and T. J. WHITE. 1972. Photoproducts of retinal photopigments and visual adaptation. *Vision Res.* **12**:805.

NOLTE, J., and J. E. BROWN. 1972. Ultraviolet-induced sensitivity to visible light in ultraviolet receptors of *Limulus*. *J. Gen. Physiol.* **59**:186.

NOLTE, J., J. E. BROWN, and T. G. SMITH. 1968. A hyperpolarizing component of the receptor potential in the median ocellus of *Limulus*. *Science* (*Wash. D.C.*). **162**:677.

PAK, W. L., and R. A. CONE. 1964. Isolation and identification of the initial peak of the early receptor potential. *Nature* (*Lond.*). **204**:836.

PAK, W. L., and T. G. EBREY. 1966. Early receptor potentials of rods and cones in rodents. *J. Gen. Physiol.* **49**:1199.

RUSHTON, W. A. H. 1961. Rhodopsin measurement and dark adaptation in a subject deficient in cone vision. *J. Physiol.* (*Lond.*). **156**:193.

RUSHTON, W. A. H. 1965. The Ferrier lecture, 1962. Visual adaptation. *Proc. R. Soc. Lond. B Biol. Sci.* **162**:20.

SCHWEMER, J., M. GOGALA, and K. HAMDORF. 1971. The ultraviolet visual pigment: photochemistry *in vitro* and *in vivo*. *Z. Vgl. Physiol.* **75**:174.

SILLMAN, A. J., W. G. OWEN, and H. F. FERNANDEZ. 1972. The generation of the late receptor potential: an excitation-inhibition phenomenon. *Vision Res.* **12**:1519.

STRATTEN, W. P., and T. E. OGDEN. 1971. Spectral sensitivity of the barnacle, *Balanus amphitrite*. *J. Gen. Physiol.* **57**:435.

TSUKAHARA, Y., and K. TASAKI. 1972. Dark recovery of ERP in isolated octopus retina. *Tohoku J. Exp. Med.* **108**:97.